ACS EARTH AND SPACE CHEMISTRY

http://pubs.acs.org/journal/aesccq

Article

Observation of N_2O_5 Deposition and $ClNO_2$ Production on the Saline Snowpack

Stephen M. McNamara, Qianjie Chen, Jacinta Edebeli, Kathryn D. Kulju, Jasmine Mumpfield, Jose D. Fuentes, Steven B. Bertman, and Kerri A. Pratt*

Cite This: *ACS Earth Space Chem.* 2021, 5, 1020−1031

Read Online

ACCESS | Metrics & More | Article Recommendations | Supporting Information

ABSTRACT: Nitryl chloride ($ClNO_2$), a precursor to highly reactive chlorine radicals and a reservoir for nitrogen dioxide (NO_2), is formed from the reaction of chloride with N_2O_5, which has a longer atmospheric lifetime during the winter. Previous field observations, modeling, and laboratory ice flow tube results led to the hypothesis that saline snow is a source of $ClNO_2$ following the deposition of dinitrogen pentoxide (N_2O_5). Due to the widespread use of road salt (primarily halite) and its deposition to the snowpack, the saline snowpack in Kalamazoo, Michigan, was investigated for the potential for direct $ClNO_2$ production following N_2O_5 deposition. Vertical gas profile and snow chamber experiments were conducted during January−February 2018 with chemical ionization mass spectrometry measurements of $ClNO_2$ and N_2O_5. The vertical gas profile measurements showed N_2O_5 and $ClNO_2$ deposition over both bare and snow-covered ground. However, positive (upward) $ClNO_2$ fluxes were only observed over the snow-covered ground, showing that the saline snowpack can serve as a source of $ClNO_2$. A fraction of the $ClNO_2$ profiles over the snow-covered ground did not exhibit gradients, indicative of a balance between $ClNO_2$ production and loss, including through hydrolysis. Exposure of local snow to synthesized N_2O_5 during chamber experiments resulted in $ClNO_2$ production that depended on the snowpack physical structure. Together, these results demonstrate a saline snowpack source of $ClNO_2$, with expected relevance to both wintertime inland and coastal regions with snow.

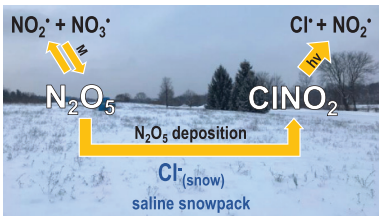

KEYWORDS: *atmosphere, chlorine, chloride, snow, winter, NO_x*

Downloaded via UNIV OF MICHIGAN ANN ARBOR on December 31, 2021 at 04:28:39 (UTC).
See https://pubs.acs.org/sharingguidelines for options on how to legitimately share published articles.

1. INTRODUCTION

Atmospheric nitryl chloride ($ClNO_2$) is a reservoir for highly reactive chlorine atoms (Cl).[1] Atomic Cl can accelerate the oxidation of volatile organic compounds, especially alkanes,[2,3] altering atmospheric composition.[1] $ClNO_2$ photolysis following sunrise also releases nitrogen dioxide (NO_2), which contributes to nitrogen oxide (NO_x = NO + NO_2) pollution and ozone (O_3) formation.[1,4] At night, $ClNO_2$ forms through the multiphase reaction of chloride (Cl^-) with dinitrogen pentoxide (N_2O_5), produced when NO_2 combines with the nitrate radical (NO_3) in the presence of a third molecule (e.g., N_2) to quench the reaction.[1] This mechanism is shown in reactions R1−R3

$$NO_2 + NO_3 + M \rightleftharpoons N_2O_5 + M \quad \text{(R1)}$$

$$N_2O_5 + Cl_{(aq)}^- \rightarrow ClNO_2 + NO_{3(aq)}^- \quad \text{(R2)}$$

$$ClNO_2 + h\nu \rightarrow Cl + NO_2 \quad \text{(R3)}$$

Numerous observations of $ClNO_2$, at levels reaching over 1 part per billion (ppb, nmol mol^{-1}), have been reported near coastal urban areas with NO_x pollution and where the primary source of chloride is sea spray aerosol.[1,5−11] $ClNO_2$ has also been observed inland at locations including Calgary, Alberta,[12,13] Boulder, Colorado,[14] and Ann Arbor, Michigan,[15] far from the influence of sea spray. Road salt aerosols,[15] playa dust,[16] and power plant plumes[17] have been shown as effective chloride-containing reaction surfaces for $ClNO_2$ production.

In addition to aerosol particles, other surfaces have been the subject of recent $ClNO_2$ research. Observations by Kim et al.[18] showed that the ocean surface is a net sink for both N_2O_5 and $ClNO_2$, despite the presence of chloride in the sea surface microlayer. The presence of chloride in "urban grime" films on buildings, sidewalks, and other surfaces is a hypothesized, but untested, source of $ClNO_2$ production.[19,20] In the laboratory, Lopez-Hilfiker et al.[21] demonstrated $ClNO_2$ production from chloride-doped ice (at temperatures ranging from −48 to −24 °C) following N_2O_5 reaction, building on lower temperature ice studies by Tolbert et al.[22] and Leu.[23] The deposition of sea salt aerosol on coastal snowpacks results in significant chloride levels.[24,25] Previous studies have shown that the Arctic snowpack is a source of trace halogen gases, including molecular bromine (Br_2),[26,27] chlorine (Cl_2),[27] bromine

Received: November 19, 2020
Revised: March 26, 2021
Accepted: March 30, 2021
Published: April 12, 2021

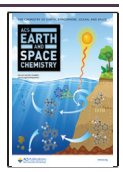

ACS Publications

© 2021 American Chemical Society

chloride (BrCl),[27] and iodine (I_2),[28] due to the concentration of solutes within the snow grain disordered interface.[29] In recent observations, McNamara et al.[30] hypothesized that N_2O_5 reacts on the surface of the Arctic snowpack to produce $ClNO_2$. The snowpack has been shown to be a significant sink of N_2O_5 in Fairbanks, Alaska, where the aerosol surface area concentrations alone were unable to explain the observed rapid losses of N_2O_5 near the snow surface.[31−33] However, to our knowledge, measurements of N_2O_5 surface deposition followed by snowpack $ClNO_2$ production have not yet been reported.

The widespread practice of road salting for deicing also occurs during the winter around the world, adding tens of millions of tons of chloride salts into the environment.[34−38] In addition to direct deposition next to roadways,[39−41] road salts are aerosolized mechanically by vehicular traffic,[42] leading to enhancements in $PM_{2.5}$ (particulate matter < 2.5 μm in diameter) levels that can be comparable to coastal sea spray-influenced areas.[35] Significant road salt mass is deposited on snowpacks hundreds of meters from roadways.[43] In both Calgary, Alberta,[12,13] and Ann Arbor, Michigan,[15] elevated atmospheric $ClNO_2$ mole ratios were observed during the winter/early spring months when road salting was abundant, with much lower $ClNO_2$ levels observed in the fall. In Ann Arbor, road salt aerosol was identified as the dominant chloride-containing aerosol source leading to $ClNO_2$ production.[15] The recent one-dimensional modeling by Wang et al.[44] suggested that $ClNO_2$ can be effectively produced at the saline, urban snowpack surface.

The assessment of $ClNO_2$ sources and sinks in cold, urban environments is important for improving our understanding of wintertime air quality.[1] N_2O_5 has a longer lifetime against thermal dissociation at lower temperatures.[45] This promotes $ClNO_2$ formation during the winter[4] and subsequent Cl radical production upon photolysis. As compared to the main atmospheric oxidant, the hydroxyl radical (OH), these Cl radicals can have higher reaction rate coefficients for alkanes and aromatics in particular.[46,47] Global model simulations predict significant losses of ethane, propane, and acetone, in particular from inclusion of Cl radical reactions.[48] The relative importance of Cl radicals is increased during the winter[49] when OH is typically less abundant due to reduced water vapor concentrations and actinic light required for OH formation.[50] Recent studies, however, suggest that HONO can be a significant wintertime OH source.[51−53] Numerical modeling studies of the wintertime urban atmosphere showed that the presence of $ClNO_2$ significantly accelerated volatile organic carbon oxidation, impacting simulated ozone and secondary organic aerosol formation.[53]

To test the hypothesis that N_2O_5 deposition on the saline snowpack can support $ClNO_2$ production, we conducted chemical ionization mass spectrometry measurements of N_2O_5 and $ClNO_2$ in Kalamazoo, Michigan, during January−February 2018. Through near-surface vertically resolved measurements, and together with measurements of atmospheric stability, we calculated $ClNO_2$ and N_2O_5 fluxes above the snow-covered and non-snow-covered ("bare" grass-covered) ground. We also conducted chamber experiments, during which local snow was exposed to synthesized N_2O_5, resulting in $ClNO_2$ production. This unique data set provides an investigation into the wintertime production of $ClNO_2$, an important reservoir species responsible for altering atmospheric oxidation.

2. EXPERIMENTAL SECTION

2.1. $ClNO_2$ and N_2O_5 Measurements Using Chemical Ionization Mass Spectrometry. $ClNO_2$ and N_2O_5 were measured during vertical gas profile and snow chamber experiments using a chemical ionization mass spectrometer (CIMS, THS Instruments, Atlanta, GA)[30,54] housed in a mobile laboratory trailer on the campus of Western Michigan University in Kalamazoo, Michigan (42.2784°N, 85.6105°W). These experiments, described in Sections 2.2 and 2.3, respectively, were conducted between January 25 and February 22, 2018, as part of the SNow and Atmospheric Chemistry in Kalamazoo (SNACK) field campaign.[51] The sampling site (Figure S1) was positioned downwind (with respect to the dominant southwest winds) of an ∼200 m long field and ∼80 m from a regularly salted major roadway.

In the CIMS, ambient trace gases can react with $I(H_2O)_n^-$ reagent ions, forming iodide adducts that are isolated with a quadrupole mass analyzer.[54] Air was pulled at 2.8 L min^{-1} (for snow chamber experiments) or 6.6 L min^{-1} (for vertical gas profile experiments) into a custom three-way valve[54] for calibration and background measurements. The CIMS ion−molecule reaction region (IMR) sampled 0.9 L min^{-1} of the inlet flow and was held at a constant pressure of 15.5 Torr. An O_3 monitor (model 205, 2B Technologies, Boulder, CO) sampled 1.7 L min^{-1} of the inlet flow, with the remaining flow dumped to exhaust. The $I(H_2O)_n^-$ reagent ions were produced by passing methyl iodide, carried in nitrogen (N_2) at 3.0−3.5 L min^{-1}, through a polonium-210 ionizer and into the IMR. Water vapor, carried in N_2 at 0.25 L min^{-1}, was added to the IMR from a room-temperature (∼23 °C) 1 L water bubbler, as in previous work.[30] Humidifying the IMR prevented ambient water vapor from changing the CIMS sensitivity during ambient sampling.[11,30] For all experiments, $ClNO_2$ was detected as $I^{35}ClNO_2^-$ at m/z 208 and as $I^{37}ClNO_2^-$ at m/z 210, with dwell times of 1.5 and 1 s, respectively. N_2O_5 was detected as $IN_2O_5^-$ at m/z 235, with a dwell time of 1.5 s. Identification of $ClNO_2$ was confirmed by the measured isotopic ratio of $^{37}ClNO_2$ to $^{35}ClNO_2$ (averages of 0.31 and 0.32 for vertical profile and snow chamber experiments) compared to the theoretical ratio of 0.3200 (Figure S2).[55] Nitric acid (HNO_3) and molecular chlorine (Cl_2) were also monitored at m/z 190 ($IHNO_3^-$) and m/z 197 and 199 (ICl_2^-), respectively. Background measurements were conducted by passing the airflow through a scrubber with two sections consisting of glass wool and 120 °C-heated stainless-steel wool, respectively, removing $ClNO_2$ and N_2O_5 with 90 ± 4 and 94 ± 4% efficiencies, respectively (Figure S3).

Online calibrations using Cl_2 were conducted at the beginning and end of each vertical profile and snow chamber experiment by adding 0.2 L min^{-1} of 12 and 29 ppb Cl_2 (in N_2), respectively, to the CIMS inlet flow from a permeation source (VICI). The permeation rate was verified daily by reacting permeated Cl_2 in N_2 with 2% potassium iodide in a glass impinger and measuring the absorbance of the oxidation product, triiodide, with UV−visible spectrophotometry at 352 nm.[54] $ClNO_2$ and N_2O_5 were calibrated offline using sensitivities relative to Cl_2 at m/z 197: 3.7 ± 0.4 for $ClNO_2$ (m/z 208) and 0.85 ± 0.08 for N_2O_5 (m/z 235); the calibration methods are described elsewhere.[15,30] The 3σ limits of detection (LODs) during the vertical profile experiments, corresponding to 1 min background periods, were 0.7 ppt for $ClNO_2$ and 2 ppt for N_2O_5, with respective measurement

https://doi.org/10.1021/acsearthspacechem.0c00317
ACS Earth Space Chem. 2021, 5, 1020−1031

uncertainties of 22% + 0.7 ppt and 25% + 2 ppt. For the snow chamber experiments, the 3σ LOD for $ClNO_2$, corresponding to 2 min background periods, was 0.3 ppt, with a measurement uncertainty of 20% + 0.3 ppt. All mole ratios are reported with the propagated measurement uncertainty unless stated otherwise (e.g., 95% confidence intervals for averages). Ambient Cl_2 was not observed above the 3−5 ppt CIMS detection limits during the vertical profile and snow chamber experiments.

2.2. Vertical Gas Profile Experiments. Vertical gas profile experiments were conducted on 11 nights, typically starting after 20:00 eastern standard time (EST), following sunset (∼17:45−18:30) and ending before sunrise (∼07:30−08:00 EST), for a total of 42 profiles of $ClNO_2$ and N_2O_5. Table S1 provides the experiment details, including the times, ground cover, and corresponding meteorological conditions. $ClNO_2$ and N_2O_5 were observed above the CIMS detection limits for all experiments. Air was pulled into the CIMS inlet through a 30 °C heated and insulated, 4.5 m long, 0.95 cm i.d. FEP tube that was attached to the custom three-way valve (Section 2.1) for a total residence time of 2.9 s through the air sampling line. Over the course of an experiment, the outside end of the sampling line was placed at multiple heights between 3 and 152 cm above the ground level (agl), with intervals of typically less than ∼25 cm. The duration of each experiment ranged from 20 to 90 min, with sampling at five to eight heights for 2−8 min each. The full gas profile was repeated up to six times throughout the night. CIMS background measurements (Section 2.1) were taken at the beginning and end of each height measurement or at the beginning and end of an experiment.

To avoid systematic biases due to temporal trends, the order of the sampling heights was randomized except for the highest sampling level (122−152 cm agl, depending on the snow depth), which was always sampled at the beginning and end of each profile. Despite the randomized sampling, $ClNO_2$ and N_2O_5 mole ratios would occasionally exhibit an overall downward or upward trend during an experiment due to changing atmospheric composition over the course of a 20−90 min vertical profile experiment. The vertical gradient mole ratios were corrected using the detrending algorithm described in Section S1 to prevent the temporal variations from impacting the magnitude and direction of the resulting flux.

The CIMS sampling line was flushed with Milli-Q water (18.2 MΩ cm and <3 ppb total organic carbon) and dried with ultrapure N_2 (Metro Welding Supply) before every vertical gas profile to prevent the buildup of contaminants on the line walls. The sampling line was characterized post-campaign for wall losses of N_2O_5 and $ClNO_2$. Constant flows of N_2O_5 and $ClNO_2$ were generated following the same procedures as those for the calibrations,[15,30] and each was introduced separately to the end of the sampling line while pulling room air at the same total flow rate (6.6 L min^{-1}) as that of the campaign. The sampling line was then bypassed, and N_2O_5 and $ClNO_2$ were individually sent into the calibration port to achieve control measurements from which the line measurements were subtracted. The wall losses were determined to be 10% for N_2O_5 and 20% for $ClNO_2$, which were within measurement uncertainties of our previous work.[15] The ambient vertical profile data reported here were corrected for these losses. When vertical profile or snow chamber experiments were not being performed, ambient N_2O_5 and $ClNO_2$ were measured using a ring torus inlet, designed and previously shown to minimize wall losses.[54,56,57] As shown in Figure S4 for the representative evening of January 30−31, the mole ratios measured during the vertical profile experiments follow the same temporal trend as that of the data collected using the ring torus inlet, consistent with minimal line artifacts.

Fluxes of $ClNO_2$ and N_2O_5 were calculated using the gradient method (E1).[58−60]

$$\text{Flux} = -K_c \frac{dC}{dz} \tag{E1}$$

dC/dz is the change in the concentration (C) of $ClNO_2$ or N_2O_5 as a function of height (z) and K_c (m^2 s^{-1}) is the atmospheric eddy diffusivity for $ClNO_2$ or N_2O_5. The concentration gradient dC/dz is calculated as

$$\frac{dC}{dz} \approx \frac{C_1 - C_0}{z_1 - z_0} \tag{E2}$$

where C_1 and z_1 are the concentration (in molecules cm^{-3}) and height (in cm agl) at the tallest sampling height (122−152 cm), respectively, and C_0 and z_0 are the concentration and height at the lowest sampling height (∼3 cm agl), respectively. Uncertainties can arise in the gas flux calculation when using the lower intake close to the surface of interest due to the air turbulence "near-field effects".[60] Therefore, the derived fluxes are likely the upper (absolute) limits. The K_c is related to the eddy diffusivity for the momentum (K_m) through $K_c = K_m/S_c$, where S_c is the Schmidt number for $ClNO_2$ (1.2 at 0 °C and 1 atm) or N_2O_5 (1.6 at 0 °C and 1 atm).[61,62] K_m is calculated as[63]

$$K_m = \frac{\kappa z_s u^*}{\phi_m} \tag{E3}$$

where κ is the von Kármán constant (0.4), z_s is the logarithmic mean sampling height (in m agl), ϕ_m (2 ± 1, on average for the nighttime experiments) is the normalized wind shear function to consider the influences of atmospheric stability,[63−65] and u^* (in m s^{-1}) is the friction velocity, determined by concurrent measurements of three-dimensional (3-D) wind speed during the vertical profile experiments. Throughout the SNACK campaign, a non-orthogonal, 3-D sonic anemometer (model CSAT3, Campbell Scientific Inc., Logan, UT) positioned at 1.4 m agl made 20 Hz measurements of the sonic air temperature (T_{air}) and 3-D wind speed (u = zonal wind speed, v = meridional wind speed, and w = vertical wind speed). Due to the sonic anemometer's position near the upper height of the vertical profiles, K_m was scaled down to the midpoint height of the gas profile measurements (halfway between the upper and lower measurement heights, which fluctuated based on the snow depth), assuming K_m varies linearly with height within the atmospheric surface.[66] Based on turbulent covariance of the 3-D wind speed (30 min averaged), u^* was calculated according to E4

$$u^* = \sqrt[4]{\overline{u'w'}^2 + \overline{v'w'}^2} \tag{E4}$$

where u', v', and w' are fluctuations about the mean wind speed. For negative (deposition) fluxes, N_2O_5 and $ClNO_2$ deposition velocities (cm s^{-1}) were calculated as the flux divided by the N_2O_5 or $ClNO_2$ concentration at the height closest to the midpoint of the vertical gas profile, which was typically 55−85 cm agl.

A fraction of the profiles was disqualified due to meteorology or excessive uncertainty, as discussed in detail in Section S1

https://doi.org/10.1021/acsearthspacechem.0c00317
ACS Earth Space Chem. 2021, 5, 1020−1031

and Figure S5. In total, 35/42 $ClNO_2$ and 25/42 N_2O_5 profiles were used to determine fluxes in this study (Table S1). The sign (+ or −) of the flux represents a source or a sink of the gas, respectively. For additional analysis, all profiles were further classified as "positive", "negative", or "no gradient", representing the net surface production, deposition, or equilibrium, respectively, based on the following criteria. In comparing the mole ratios at the highest and lowest sampling heights, positive profiles had statistically significantly ($p < 0.05$) larger mole ratios at the lowest sampling height, and negative profiles had statistically significantly larger mole ratios at the highest sampling height. No gradient profiles had no significant difference between mole ratios for the highest and lowest sampling heights. Flux uncertainties were calculated by propagating the CIMS measurement uncertainties (Section 2.1) for the highest and lowest sampling heights.

2.3. Snow Chamber Experiments. Snow chamber experiments were conducted to test the hypothesis that authentic saline snow exposed to N_2O_5 generates $ClNO_2$, as predicted from previous laboratory experiments by Lopez-Hilfiker et al.[21] These qualitative experiments were similar to previous molecular halogen and NO_x field-based snow chamber experiments by Pratt et al.[26] and Honrath et al.,[67] respectively, and the molecular halogen lab-based artificial snow chamber experiments by Wren et al.[68] As in these previous studies, the snow chamber experiments herein were not quantitative due to the inability to quantify the snow surface area and wall losses, as well as chloride contamination of the chamber. These challenges are also similar to those described by Ahern et al.[69] for chamber experiments in which biomass burning aerosol was exposed to N_2O_5 to examine $ClNO_2$ production. Therefore, we follow this previous work and obtain qualitative insights by identifying products and trends between samples. Following the methodology of Ahern et al.,[69] we report ratios of measured $ClNO_2$ during snow exposure to maximum N_2O_5 measured for the empty chamber. While the air temperatures for the empty and snow-filled chamber experiments should be similar, the residence time is longer for the empty chamber, allowing more time for N_2O_5 surface losses and $ClNO_2$ production resulting from reactions with chloride contamination. The setup limitations did not allow variation of the residence time in the chamber to assess the impact of this variable. Therefore, the ratios reported here are meant to be qualitative.

During the chamber experiments, local snow samples were exposed to synthesized N_2O_5 in the snow chamber at the SNACK field site. Snow chamber experiments were conducted on February 17 and 18, 2018, with four different snow types for a total of eight experiments. The snow samples tested included (1) Field snow, collected from the field located ∼80−100 m from the adjacent main roadway (Stadium Drive), (2) Service Road snow, collected from the small access road for the field site, which was not directly salted but was snow plowed and used by vehicles occasionally, (3) Stadium Drive snow, collected from the shoulder of the heavily traveled, regularly snow-plowed, and salted five-lane road adjacent to the site, and (4) Field + Salt, the same as (1) but with ∼10−20 g of road salt (Safe Step 3300, NaCl) crushed to a powder and spread over the top of the sample in the vessel (see Figure S1 for locations).

A schematic of the snow chamber experiment is provided in Figure S6. A 950 cm^3 borosilicate glass vessel was used as the snow chamber. Empty vessel background runs with and without N_2O_5 were also performed as controls. All samples were added to the vessel using polypropylene scoops with no packing of the snow (with the snow sample approximately filling the entire vessel). Following each sample's N_2O_5 exposure experiment, the snow chamber was washed with ultrapure water and methanol. The snow chamber was sealed with a polypropylene lid and a silicone gasket. Two 0.25 in. PFA bulkhead fittings (Swagelok) were attached to opposite corners of the lid, serving as the inlet and outlet for gases, and each extended 2.5 cm into the snow sample. The CIMS pulled on the outlet of the snow chamber at 2.77 L min^{-1} through a 30 cm long, 0.48 cm i.d. FEP Teflon tube attached to the CIMS inlet. The residence time of the empty chamber is calculated to be 20 s, with the residence time decreased when snow was present.

For introduction into the snow chamber, N_2O_5 was synthesized by combining, in a 2.2 cm i.d. PFA Teflon tube, a 1.10 L min^{-1} flow of O_3 (∼2 ppm, in excess) from an O_3 calibration source (model 306, 2B Technologies) with a 0.065 L min^{-1} flow of NO_2 from a pressurized gas cylinder (1.96 ppm in N_2, Metro Welding Supply). This N_2O_5 flow was then diluted with 1.74 L min^{-1} of dry N_2 from the headspace of a liquid N_2 dewar before entering the snow chamber at a total flow of 2.84 L min^{-1}, creating a slight pressurization of the chamber. A constant flow of N_2O_5 was sent into the snow chamber, with maximum empty chamber N_2O_5 measured to be 305 and 378 ppt on February 17 and February 18, respectively. Each snow sample was exposed to the N_2O_5-laden N_2 flow for 30−40 min until both $ClNO_2$ and N_2O_5 signals stabilized, from which these stable signals were used to calculate average mole ratios presented in this work. The experimental setup was completely covered with a tarp to prevent any interaction with solar radiation. For all experiments, Cl_2 was not observed above its detection limit (3−5 ppt), and the HNO_3 signal was not elevated between the blank and N_2O_5-doped runs, suggesting minimal influence from reactions on the chamber walls.

2.4. Snow Physical and Chemical Measurements. Snow samples were collected during most snow chamber and vertical gas profile experiments. For the vertical gas profile experiments, surface snow (top 1−2 cm) samples from the sampling site were typically collected after the final profile measurement on a given night (Table S2). For most snow chamber experiments, samples were collected before and after addition to the snow chamber vessel and exposure to N_2O_5 (Table S3). The snowpack density was measured using a snow density gauge (Scientist 200, Brooks Range Inc.), and the grain sizes for the snow chamber samples were estimated using a snow grid card (Brooks Range Inc.) with 1, 2, and 3 mm grid sizes. Snow samples were analyzed post-campaign for the inorganic ion composition using ion chromatography (IC, Dionex ICS-1100 for cations and Dionex ICS-2100 for anions). We report snowmelt concentrations of sodium (Na^+), potassium (K^+), magnesium (Mg^{2+}), calcium (Ca^{2+}), chloride (Cl^-), and nitrate (NO_3^-). The snow collection, sample handling, and IC methods were as described by Chen et al.[51] For the snow chamber experiments, snow samples collected before and after N_2O_5 addition showed some variability in snowmelt inorganic ion concentrations, but not in a systematic manner, suggesting greater variability within the larger snow sample used (Table S3). The data for the snow samples following exposure to N_2O_5 are discussed in Section 3.3.

https://doi.org/10.1021/acsearthspacechem.0c00317
ACS Earth Space Chem. 2021, 5, 1020−1031

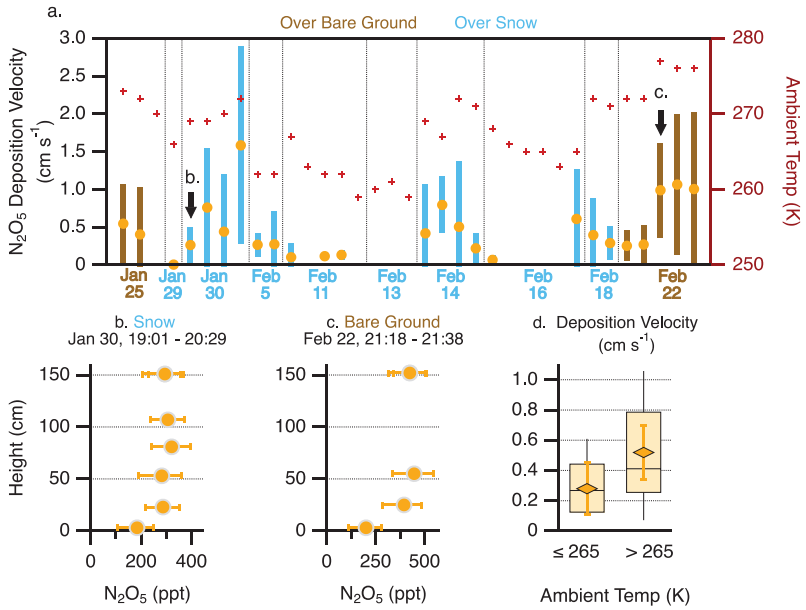

Figure 1. (a) Average ambient temperatures and N_2O_5 deposition velocities, with error bars representing propagated uncertainties, determined for each of the 25 N_2O_5 vertical gas profile experiments, over snow-covered (blue) and bare (brown) ground surfaces, from January 25 to February 22, 2018, in Kalamazoo, Michigan. Black arrows point to example N_2O_5 profiles over (b) snow on January 30 and (c) bare ground on February 22. (d) Box and whisker plots showing the distributions (90th/10th and 75th/25th percentiles and medians) of the N_2O_5 deposition velocities when the ambient temperatures were ≤265 and >265 K. The diamonds represent the average deposition velocities, with 95% confidence intervals, in each bin. The averages are statistically significantly different at the 90th confidence interval (p = 0.08).

3. RESULTS AND DISCUSSION

3.1. Bare Ground and Snow-Covered Ground Are a Sink for N_2O_5. During all vertical gas profile experiments, N_2O_5 was observed from near the ground/snow level to 1.5 m. This follows wintertime observations of N_2O_5 at 12 m agl from a 2016 campaign in Ann Arbor, Michigan, a comparable urban location with a relatively flat terrain.[15] Here, the vertical N_2O_5 gradient measurements at multiple heights up to 1.5 m agl show that the bare and snow-covered ground are both sinks for N_2O_5 (Figure 1). On average, N_2O_5 mole ratios were ∼60 ppt lower at the surface (90 ± 10 ppt at ∼3 cm agl) compared to those at ∼1.5 m (149 ± 9 ppt). For both bare and snow-covered ground conditions, N_2O_5 mole ratios decreased toward the surface, consistent with numerous previous measurements of near-surface N_2O_5 profiles.[18,32,70,71] During the vertical gas profile experiments, the average N_2O_5 mole ratios at the top vertical profile height were similar over both the bare and snow-covered ground (150 ± 90 and 150 ± 50 ppt, respectively). All N_2O_5 profiles and atmospheric stability data (eddy diffusivity, friction velocity, and air temperature) are shown in Figures S7−S12. The average N_2O_5 flux derived from all 25 vertical profile experiments was $-(2.8 \pm 0.9) \times 10^9$ molecules cm^{-2} s^{-1}, indicating a net downward flux of N_2O_5 to the surface (deposition), consistent with the profile showing decreasing N_2O_5 mole ratios within 10 cm above the snowpack surface. The average N_2O_5 fluxes over snow, $-(2 \pm 1) \times 10^9$ molecules cm^{-2} s^{-1}, and bare ground, $-(4 \pm 2) \times 10^9$ molecules cm^{-2} s^{-1}, were not statistically significantly different (p = 0.48), showing net N_2O_5 deposition regardless of ground cover.

Given the downward flux of N_2O_5, it is useful to consider its deposition velocity, defined as the flux divided by the average N_2O_5 concentration, for comparison to other studies. The campaign average N_2O_5 deposition velocity was 0.5 ± 0.1 cm s^{-1}. For the seven gas profiles over the bare ground, the average N_2O_5 deposition velocity (0.6 ± 0.3 cm s^{-1}) was not significantly different (p = 0.16) from the average of 18 N_2O_5 profiles over snow (0.4 ± 0.2 cm s^{-1}). Huff et al.[32] previously determined N_2O_5 deposition velocities to be 0.6 ± 0.5 cm s^{-1} over snow in Fairbanks, Alaska, during November 2009, in line with our results over snow and bare ground in Kalamazoo.

In considering the deposition of N_2O_5, it is important to consider wintertime near-surface processes. While microbial activity in soil can be a NO_x source, particularly under warm conditions, Seok et al.[72] reported NO_x measurements in a northern Michigan forest from November to April and did not observe a measurable NO flux. In addition, Seok et al.[72] reported no significant difference in NO or O_3 mole ratios between natural and Tedlar-covered plots, used to isolate the snowpack from the soil. Previous Arctic snowpack measurements showed low O_3 deposition velocities on the order of 0.01 cm s^{-1}.[73] During the northern Michigan study by Seok et al.,[72] a positive NO_2 flux was only observed during the daytime when snow was present due to snowpack nitrate (NO_3^-) photolysis, as observed previously in northern Michigan.[67] While NO_x measurements were not conducted during the SNACK campaign, photochemical snowpack NO_x production is expected and consistent with the observed daytime HONO production, attributed to snowpack nitrate photolysis, during the SNACK campaign in Kalamazoo.[51] However, the current work focuses on dark processes. While the snowpack is known to be a source and a sink of trace gases,[74] the snowpack surface is not known to be an aerosol source, unlike the seawater surface, suggesting that increased aerosol concentrations near the snowpack surface are unlikely. In this work, the loss of N_2O_5 near the snowpack surface was investigated in the context of $ClNO_2$ production from the saline snowpack, as discussed in the following sections.

https://doi.org/10.1021/acsearthspacechem.0c00317
ACS Earth Space Chem. 2021, 5, 1020−1031

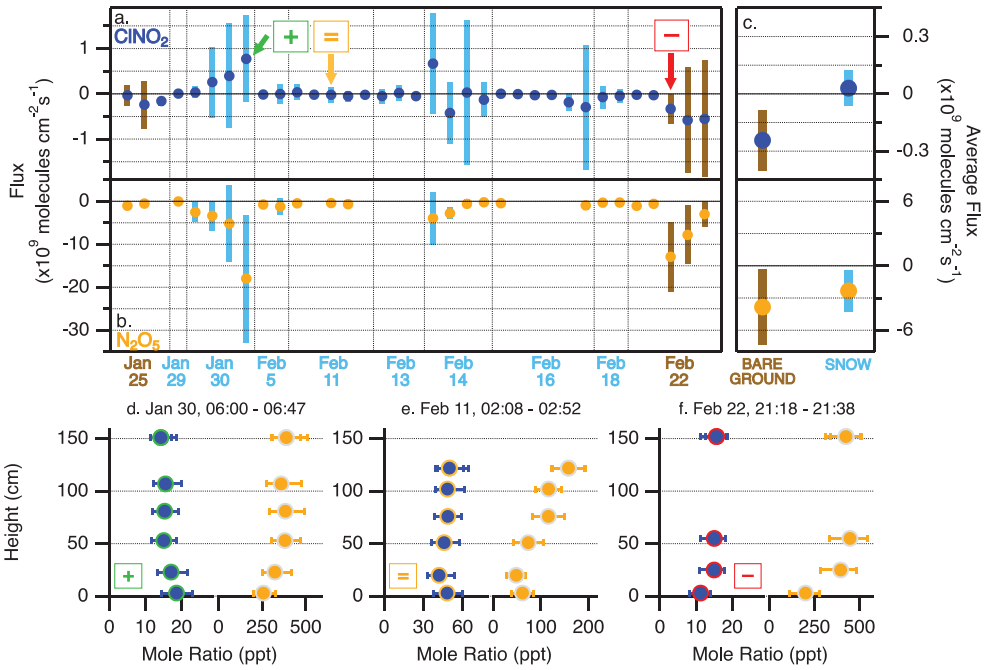

Figure 2. Fluxes of $ClNO_2$ (a) and N_2O_5 (b) over the bare ground and snowpack from January 25 to February 22, 2018. Error bars represent propagated uncertainties. (c) Average $ClNO_2$ and N_2O_5 fluxes, with 95% confidence intervals, over bare ground and snow. The average $ClNO_2$ fluxes above the bare ground and snow were statistically significantly different (p = 0.01), but the corresponding average N_2O_5 fluxes were not significantly different (p = 0.48). Example positive (+, d), no gradient (=, e), and negative (−, f) $ClNO_2$ profiles on January 30, February 11, and February 22, respectively, are shown. All flux values and weather conditions for the vertical gas profile experiments are provided in Table S1.

The observed N_2O_5 deposition velocities in Kalamazoo are aligned with the recent numerical modeling by Wang et al.[44] of N_2O_5 and $ClNO_2$ during February−March 2016 in Ann Arbor, Michigan. In that prior work, the N_2O_5 deposition velocities over snow were calculated to increase from 0.23 cm s^{-1} at ∼258 K to 1.06 cm s^{-1} at 272−280 K. At the higher temperatures, 95% of N_2O_5 was simulated to undergo hydrolysis following deposition.[44] Our measurements in Kalamazoo generally followed the predictions of the Wang et al.[44] modeling; the average N_2O_5 deposition velocity at 265 K and lower was 0.3 ± 0.2 cm s^{-1}, compared to the average of 0.5 ± 0.2 cm s^{-1} (significantly different at p = 0.08) for warmer (>265 K) conditions (Figure 1). Increased atmospheric mixing is expected with higher temperatures,[66] as was indeed the case for this study (Figure S7). In addition, as the temperature of the snowpack increases, more liquid water is present at the snow grain surface,[75] increasing the likelihood of N_2O_5 hydrolysis versus reaction with Cl^- to produce $ClNO_2$.[44,76]

3.2. Vertical Gradient Measurements Indicate That the Snowpack Can Be a Source of $ClNO_2$. In contrast to the N_2O_5 profiles, not all $ClNO_2$ profiles decreased as a function of height near the surface and instead varied throughout the study (Figure 2, Table S1). For example, on January 30 over light snow coverage, $ClNO_2$ mole ratios increased near the surface, exhibiting an upward net flux. Positive $ClNO_2$ profiles (six total), which increased near the surface, were only observed over the snow-covered ground. Between February 5 and 18 over a thick snowpack, 45% of $ClNO_2$ profiles during this period (10 of 22) exhibited no gradient, with similar mole ratios throughout the profile (Figure 2). Profiles without significantly changing $ClNO_2$ mole ratios from the surface to the top height are indicative of a balance between $ClNO_2$ production and loss, which can be explained by recent modeling suggesting that the magnitude of the $ClNO_2$ snowpack flux depends on whether $ClNO_2$ formed undergoes hydrolysis or is released to the overlying air.[44] For the eight profiles over the bare ground, seven had decreasing $ClNO_2$ mole ratios near the surface (negative profiles) and one (on January 25) showed no gradient (Table S1). Prior to the January 25 bare ground neutral $ClNO_2$ profile, light snow and a wintry mix were observed on January 23−24, likely prompting road salting; thus, the January 25 profile may have been influenced by the deposited salt on the ground, serving as a minor source of $ClNO_2$. Therefore, the vertical gradient profiles support the surface as both a source and a sink of $ClNO_2$, as proposed previously through numerical modeling by Wang et al.[44]

Consistent with the observed vertical profiles, the $ClNO_2$ fluxes were highly variable from -6×10^8 to $+8 \times 10^8$ molecules cm^{-2} s^{-1}, unlike the N_2O_5 fluxes, which were consistently negative (Figure 2 and Table S1). These results emphasize that the relative contributions of the surface as a source versus sink of $ClNO_2$ vary with time. However, it is important to note that these vertical gradient fluxes have high uncertainties and represent upper (absolute) values based on the measurement methodology. On average, during the vertical gas profile experiments, the $ClNO_2$ mole ratios at the top vertical profile height were similar at the 95% confidence level over the snow-covered ground (27 ± 7 ppt) and the bare ground (18 ± 8 ppt). For the profiles with negative fluxes, the average $ClNO_2$ deposition velocity was calculated to be 0.14 ± 0.07 cm s^{-1}, smaller than that of N_2O_5 (0.5 ± 0.1 cm s^{-1}), consistent with the ground surface as both a source and a sink of $ClNO_2$. Overall, the average $ClNO_2$ flux over the snow-covered ground, $+(3 \pm 14) \times 10^7$ molecules cm^{-2} s^{-1}, was statistically significantly (p = 0.01) more positive than the average flux over the bare ground, $-(24 \pm 23) \times 10^7$ molecules

https://doi.org/10.1021/acsearthspacechem.0c00317
ACS Earth Space Chem. 2021, 5, 1020−1031

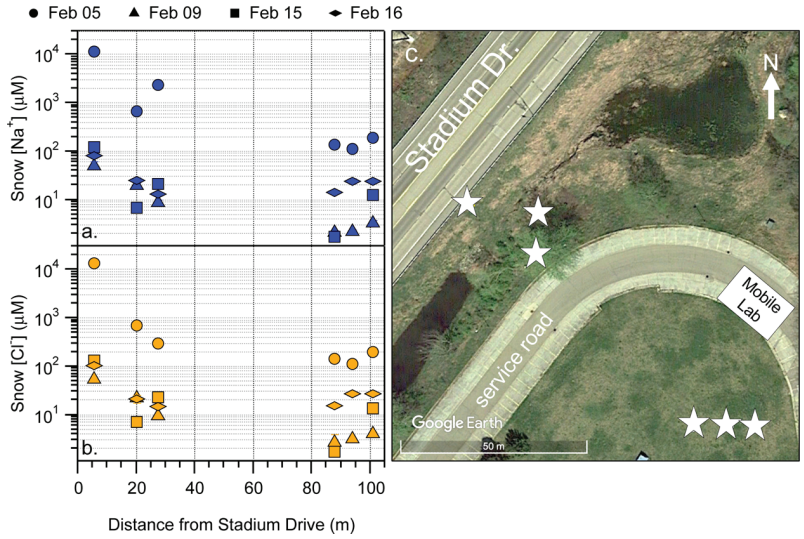

Figure 3. Bulk snowmelt Na^+ (a) and Cl^- (b) concentrations of surface (top 1−2 cm) snow samples collected during February 2018 at various distances from the major roadway (Stadium Drive) that was regularly salted. Error bars, typically smaller than the markers, represent 1σ (N = 3 trials for each sample). (c) Map of the field site, with stars representing the snow sampling locations. The Service Road, on which the mobile laboratory was deployed, experienced only occasional motor vehicle traffic and was minimally snow-plowed but not salted. Imagery and map data were adapted from Landsat/Copernicus and Google Earth, respectively. Copyright 2020.

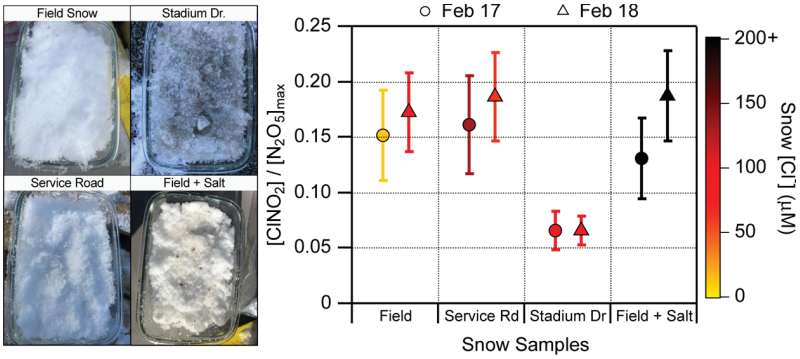

Figure 4. Snow chamber experiments were conducted on February 17 and 18, 2018, with photographs shown (left) of the snow samples: Field, Service Road, Stadium Drive, and Field + Salt, as described in Section 2.3. (Right) Average $ClNO_2$ mole ratios, measured following the N_2O_5 addition into the snow chamber for each the four snow samples, divided by the maximum measured N_2O_5 mole ratios measured for the empty chamber on each day (305 and 378 ppt on Feb 17 and 18, respectively). Error bars represent the propagated CIMS measurement uncertainties. The color scale represents the measured bulk snow [Cl^-]. The [Cl^-] of the Field + Salt samples on February 17 and 18 were 5.1 and 2.6 M, respectively, and are shown off scale for clarity.

cm^{-2} s^{-1} (Figure 2). This further indicates that the snowpack can be a source of $ClNO_2$ following N_2O_5 deposition.

The field site was influenced from nearby road salt deicing, adding chloride salts to the snowpack (Figure 3). The site was bounded by Stadium Drive, a road that experienced an annual average daily traffic volume of 22,594 vehicles in 2018[77] and was regularly deiced with chloride-containing road salt during the winter. The city of Kalamazoo uses primarily NaCl for deicing, with $CaCl_2$ added for lower temperature periods, and Western Michigan University uses NaCl coated in beet juice for deicing. This is consistent with the local snowmelt composition showing significant sodium (Na^+) and chloride (Cl^-) concentrations, as well as varying amounts of calcium (Ca^{2+}), magnesium (Mg^{2+}), and potassium (K^+) (Tables S2 and S3). Previous studies have shown that vehicular traffic aerosolizes road salt,[42] with the largest particles depositing within hundreds of meters from the salted roadway.[39,40,43] This explains the enhancements in sodium (Na^+) and chloride (Cl^-) concentrations for surface snow samples collected in the closest 5−30 m to Stadium Drive (up to 11.4 ± 0.2 mM Na^+ and 13.24 ± 0.08 mM Cl^- (±1σ) on February 5) versus up to 0.188 ± 0.002 mM Na^+ and 0.196 ± 0.002 mM Cl^- at 101 m away from the road (Figure 3). Daily variability was observed, with lower salt concentrations for fresh snowfall (February 9) and above-freezing temperatures (February 15−16) compared to that of older snow (February 5) (Figure 3). Therefore, $ClNO_2$ produced from the snowpack was likely the result of N_2O_5 reaction with chloride from road salt aerosol deposition.

While the $ClNO_2$ fluxes were highly variable (−6 × 10^8 to +8 × 10^8 molecules cm^{-2} s^{-1}) (Figure 2 and Table S1), they were not correlated with bulk [Cl^-] or [NO_3^-] in the surface snow samples collected at the site during the vertical profile experiments (Table S2). This suggests that the $ClNO_2$ production is not limited by these bulk ion concentrations in this snowpack. Nitrate is a product of N_2O_5 hydrolysis that suppresses the N_2O_5 uptake onto particles,[78,79] while chloride is required for $ClNO_2$ production.[80] Chloride and nitrate are expected to be enriched within brine pockets on the snow

https://doi.org/10.1021/acsearthspacechem.0c00317
ACS Earth Space Chem. 2021, 5, 1020−1031

grain surface.[81,82] Model simulations by Wang et al.[44] for Ann Arbor, MI, also suggested that the snowpack $ClNO_2$ flux is dependent on the temperature due to changes in the snow surface brine fraction, with more $ClNO_2$ lost to hydrolysis at higher temperatures, leading to a more negative (downward) flux. Although the experimental $ClNO_2$ fluxes in this study showed no correlation with the air temperature, transformations in the snowpack morphology, caused by melting and/or re-freezing,[83] likely impacted $ClNO_2$ production as this decreases the available surface area for multi-phase reactions.[84,85] This motivated snow chamber experiments in which snow samples of differing physical and chemical properties were exposed to N_2O_5, and resulting $ClNO_2$ was monitored (Section 3.3).

3.3. $ClNO_2$ Production during Snow Chamber Experiments. Snow chamber experiments were conducted to further test the hypothesis that authentic saline snow exposed to N_2O_5 generates $ClNO_2$, as predicted from previous laboratory experiments by Lopez-Hilfiker et al.[21] During the snow chamber experiments, local snow samples were exposed to synthesized N_2O_5 in the snow chamber at the SNACK field site. As in previous snow chamber studies,[26,67,68] yields should not be derived from the experiments due to the inability to quantify the snow surface area and chamber wall losses, as well as the chloride contamination of the chamber, as discussed in Section 2.3. Following the method of Ahern et al.,[69] who examined $ClNO_2$ production from biomass burning aerosol within a chamber, we present ratios of average $ClNO_2$ measured for a given snow sample to the maximum measured N_2O_5 for the empty chamber on each day, ($[ClNO_2]/[N_2O_5]_{max}$), for comparison of the relative differences between the snow samples.

Four different surface snow samples, Field, Service Road, Stadium Drive, and Field + Salt, pictured in Figure 4 and listed in Table S3, were exposed to a constant flow of N_2O_5 during two sets of experiments on February 17 and 18. The bulk $[Cl^-]$ of the Field, Service Road, and Stadium Drive snow samples (no additional salt added) ranged from 12 to 130 μM (Figure 4). The Field and Service Road snow samples were relatively fine (<1 mm grain size, similar to fresh snowfall) and did not appear melted. In contrast, the Stadium Drive sample was previously melted and re-frozen, consisting of larger ice pellets up to ∼3 mm in diameter. While the snow nearest to the roadway was typically the highest in bulk $[Cl^-]$, as observed on February 5 (Figure 3), the Stadium Drive snow sample chloride concentrations were unexpectedly low (83−92 μM). However, from February 14 to 18, above-freezing air temperatures led to snowmelt, causing ions to flow out from the surface snow with the meltwater and lower the snow inorganic ion concentrations.[86,87] This washout effect was likely the greatest for the Stadium Drive snow due to increased melting from the freezing point depression associated with the originally higher chloride concentrations. This is also consistent with the freeze−thaw morphology of the Stadium Drive snow, compared to the fine snow grains of the Field and Service Road snow samples. To examine the impacts of the morphology and chloride concentration, snowmelt was induced with the addition of 10−20 g of crushed road salt to the Field snow (thereby called the Field + Salt snow sample). For all samples, $ClNO_2$ was observed following the addition of N_2O_5 to the snow chamber (Figure 4). Cl_2 was not measured above the 3−5 ppt detection limit. This result is consistent with the laboratory experiments by Lopez-Hilfiker et al.[21] involving the N_2O_5 uptake on saline ice, which showed only $ClNO_2$ production.

For both sets of experiments on February 17 and 18, the bulk $[Cl^-]$ of the snow samples did not correlate with the levels of $ClNO_2$ produced (Figure 4). This is evident for the Field and Service Road samples, which ranged in $[Cl^-]$ from 12 to 130 μM, while producing similar levels of $ClNO_2$ (47−67 vs 49−72 ppt, respectively, given maximum measured N_2O_5 within the empty chamber of 305 and 378 ppt on Feb 17 and 18, respectively). The ratios of $[ClNO_2]/[N_2O_5]_{max}$ were 0.15−0.17 and 0.16−0.19 for the Field and Service Road samples (Figure 4). Increasing $[Cl^-]$ by several orders of magnitude (up to 5.1 and 2.6 M for February 17 and 18, respectively) with the addition of crushed road salt to the Field snow samples also did not cause a significant increase in $ClNO_2$ production. For the snow samples tested here, the bulk snowmelt $[Cl^-]$ was likely not limiting, within the time period of exposure, because $ClNO_2$ production was not sensitive to this variable. In addition, no correlation was observed with bulk snowmelt $[NO_3^-]$ (Table S3), which can suppress the N_2O_5 uptake[78,79] and is likely enriched in brine pockets at the saline ice surface.[81,82] The snow chloride concentration, however, defines the calculated snow grain brine volume fraction,[75] thereby indirectly affecting the predicted $ClNO_2$ yield. Following the methodology presented by Wang et al.,[44] we calculate the predicted $ClNO_2$ yields to range from 0.1 to 0.5 for the February 17 snow samples and from 0.3 to 0.5 for the February 18 snow samples, excluding the Field + Salt sample, for which the high $[Cl^-]$ result in calculations of 100% brine (complete snowmelt) due to freezing point depression.

The physical characteristics of the snow sample likely impacted the production of $ClNO_2$ because the available reactive surface area decreases when the snow grains begin to coagulate during and after melting and re-freezing.[84] The presence of more liquid water at the snow grain surface at higher temperatures[75] increases the likelihood of N_2O_5 hydrolysis rather than that of reaction with Cl^- to produce $ClNO_2$.[44,76] The melt onset was induced in the Field + Salt samples by the addition of crushed road salt. Twenty minutes after the salt was added, the resulting $ClNO_2$ production from the Field + Salt sample on February 17 was significantly lower than that of the Field sample (40 ± 9 vs 46 ± 9 ppt, $p = 0.02$). The $[ClNO_2]/[N_2O_5]_{max}$ ratios were not significantly different between the February 17 Field + Salt and Field samples (0.13 ± 0.04 vs 0.15 ± 0.04, Figure 4). The melting snow would reduce the snow grain surface area and increase the snow grain brine volume fraction, increasing the probability of N_2O_5 hydrolysis rather than that of $ClNO_2$ production. The hydrolysis of $ClNO_2$ is a possibility,[18] especially for temperatures near 0 °C,[44] and may also explain the reduced $ClNO_2$ mole ratios observed. In comparison, for the February 18 Field + Salt sample, ∼50% less road salt was added, and the time between the addition of the road salt and the $ClNO_2$ measurement was only 12 min, thus limiting the amount of melting and likely leading to the higher $[ClNO_2]/[N_2O_5]_{max}$ ratio that was comparable to those of the frozen Field and Service Road samples (Figure 4). The role of snow grain physical characteristics may also provide an explanation for the lower $[ClNO_2]/[N_2O_5]_{max}$ ratios observed for the Stadium Drive samples, which were composed of larger ice pellets that had undergone melting and refreezing. Although not conducted simultaneously with the vertical gas profile experiments, the likely dependence of $ClNO_2$ production on

https://doi.org/10.1021/acsearthspacechem.0c00317
ACS Earth Space Chem. 2021, 5, 1020−1031

the snowpack surface area and snow grain brine volume fraction exhibited from these qualitative snow chamber experiments may explain the observation of both positive (upward) and negative (downward) $ClNO_2$ snowpack fluxes during the campaign.

4. CONCLUSIONS

Through chemical ionization mass spectrometry measurements during January−February 2018 in Kalamazoo, Michigan, N_2O_5 deposition was observed over both the bare and snow-covered ground, with average deposition velocity values (±95% confidence intervals) of 0.6 ± 0.3 and 0.4 ± 0.2 cm s^{-1}, respectively. This result is comparable to previously observed N_2O_5 deposition velocities (0.6 ± 0.5 cm s^{-1}) over snow in Fairbanks, Alaska.[32] It is also consistent with previous calculations of N_2O_5 deposition velocities (0.2−1.0 cm s^{-1}) over snow in Ann Arbor, Michigan.[44]

Deposition of $ClNO_2$ was observed over both the bare and snow-covered ground, but positive (upward) $ClNO_2$ fluxes were only observed over the snow-covered ground. The production of $ClNO_2$ from the saline snowpack is expected based on the observed N_2O_5 deposition and previous laboratory studies of $ClNO_2$ production from N_2O_5 reaction with saline ice.[21] Observed gas profiles without $ClNO_2$ gradients over the snow-covered ground are indicative of a balance between $ClNO_2$ production and loss/deposition, as predicted by recent modeling studies.[44] Notably, lower temperatures, such as those observed in the Arctic, are expected to result in greater $ClNO_2$ release to the overlying atmosphere due to reduced $ClNO_2$ hydrolysis at smaller snow grain liquid volume fractions.[44] In this study, the estimated $ClNO_2$ fluxes were highly variable, reflecting the surface as both a source and a sink of $ClNO_2$. Considering only the negative $ClNO_2$ fluxes, the average $ClNO_2$ deposition velocity was 0.14 ± 0.07 cm s^{-1}. The measurement-derived fluxes and deposition velocity can be incorporated into numerical models to assess the impact of the surface snowpack $ClNO_2$ source, as a function of altitude, as compared to aerosols, which are instead distributed throughout the troposphere. Given the high variability in $ClNO_2$ snowpack fluxes, it is expected that the importance of the snowpack as a $ClNO_2$ source also likely fluctuates.

Snow chamber experiments exposing local saline snow to synthesized N_2O_5 also showed direct observational evidence of snowpack $ClNO_2$ production. The results of these experiments, including when additional deicing salt was added, suggest that the snowpack structure influences the magnitude of the snowpack $ClNO_2$ production. However, our understanding of the availability of reactants at the ambient snow grain surface is currently limited,[29] and challenges remain in modeling the snow microphysics and associated multiphase reactions.[88] This further highlights the need for controlled laboratory experiments of the reaction of N_2O_5 with saline snow, similar to the molecular halogen studies by Wren et al.[68] It also points to the need for laboratory studies of the impact of wet metamorphism (melt-induced snow structure changes) on this heterogeneous reaction as recent laboratory work by Edebeli et al.[89] shows decreases in the ice surface reactivity of ozone with bromide with dry metamorphism (water vapor fluxes to/from the ice surface).

Due to the extensive use of road salt globally[34−38] and significant deposition onto the snowpack within hundreds of meters,[39−41,43] $ClNO_2$ production from the urban road salt-contaminated snowpack is likely widespread, with impacts on wintertime air quality. In addition, coastal snowpacks influenced by sea salt aerosol deposition,[24,25] including those in the Arctic where $ClNO_2$ has previously been observed during the spring,[30] are also hypothesized to support $ClNO_2$ production. Future work is needed to examine the role of salt-containing urban grime, on buildings, sidewalks, and other surfaces, in $ClNO_2$ production.[19,20] Eddy covariance flux measurements, such as those previously completed by Kim et al.[18] over the ocean surface, are suggested in future studies to better constrain the observed snowpack $ClNO_2$ production and its dependence on the snowpack characteristics and evaluate additional chloride-containing surfaces as potential sources.

■ ASSOCIATED CONTENT

Supporting Information

The Supporting Information is available free of charge at https://pubs.acs.org/doi/10.1021/acsearthspacechem.0c00317.

N_2O_5 and $ClNO_2$ fluxes determined during the 2018 SNACK campaign; physical and chemical properties for snow samples collected during vertical profile experiments; bulk inorganic ion concentrations for snow samples used for snow chamber experiments; overview of the field site; isotope ratio plots of signals at m/z 210 versus m/z 208 for identification of $ClNO_2$ during vertical profile and snow chamber experiments; performance of the CIMS glass wool background scrubber; comparison of N_2O_5 and $ClNO_2$ mole ratios using the sampling line versus ambient inlet; description of the vertical profile detrending algorithm; snow chamber experiment schematic; air temperatures, friction velocities, and eddy diffusivities for the vertical profile experiments; $ClNO_2$ and N_2O_5 profiles over bare ground, Jan 25−26 and Feb 22−23; $ClNO_2$ and N_2O_5 profiles over light snow coverage, Jan 29−30, 30−31, and Feb 5; $ClNO_2$ and N_2O_5 profiles over heavy snow coverage, Feb 11−12 and Feb 13; and $ClNO_2$ and N_2O_5 profiles over light−medium snow coverage, Feb 13−14, 16−17, and 18 (PDF)

■ AUTHOR INFORMATION

Corresponding Author

Kerri A. Pratt − *Department of Chemistry and Department of Earth and Environmental Sciences, University of Michigan, Ann Arbor, Michigan 48109, United States;* orcid.org/0000-0003-4707-2290; Phone: (734) 763-2871; Email: prattka@umich.edu

Authors

Stephen M. McNamara − *Department of Chemistry, University of Michigan, Ann Arbor, Michigan 48109, United States*

Qianjie Chen − *Department of Chemistry, University of Michigan, Ann Arbor, Michigan 48109, United States*

Jacinta Edebeli − *Department of Chemistry, University of Michigan, Ann Arbor, Michigan 48109, United States; Laboratory of Environmental Chemistry, Paul Scherrer Institute, Villigen 5232, Switzerland*

Kathryn D. Kulju − *Department of Chemistry, University of Michigan, Ann Arbor, Michigan 48109, United States*

https://doi.org/10.1021/acsearthspacechem.0c00317
ACS Earth Space Chem. 2021, 5, 1020−1031

Jasmine Mumpfield − *Department of Chemistry, University of Michigan, Ann Arbor, Michigan 48109, United States*
Jose D. Fuentes − *Department of Meteorology and Atmospheric Science, Pennsylvania State University, University Park, Pennsylvania 16802, United States*
Steven B. Bertman − *Institute of the Environment and Sustainability, Western Michigan University, Kalamazoo, Michigan 49008, United States*

Complete contact information is available at: https://pubs.acs.org/10.1021/acsearthspacechem.0c00317

Notes

The authors declare no competing financial interest.

■ ACKNOWLEDGMENTS

Financial support was provided by the National Science Foundation (NSF AGS-1738588 and PLR-1417914) and the University of Michigan (U-M) Rackham Graduate School. J.E. was funded by the Swiss National Science Foundation (155999). J.M. was supported by the Detroit Research Internship Summer Experience (D-RISE) program, through NSF AGS-1738588 and CHE-1305777 (Nicolai Lehnert), U-M, and Cass Technical High School. We thank Andrew Ault, Nicholas Ellsworth, and Matthew McNamara for assistance in preparing the mobile laboratory. Katheryn Kolesar is thanked for assistance with field campaign planning, and Angela Raso, Nathaniel May, Peter Peterson, Guy Burke, and Alexa Watson are thanked for field logistical support. The Facilities Management Department at Western Michigan University is thanked for providing access to the field site and electrical support. We thank Siyuan Wang (NOAA) and Cassandra Gaston (Univ. of Miami) for helpful discussions, Jesus Ruiz-Plancarte (Penn State Univ.) and Daun Jeong (Univ. of Michigan) for data analysis assistance, L. Gregory Huey and David Tanner (Georgia Inst. of Technol.) for the loan of the NO analyzer, and Tom Ryerson and Chelsea Thompson (NOAA) for the loan of the photolytic NO_2 converter used for CIMS calibrations.

■ REFERENCES

(1) Simpson, W. R.; Brown, S. S.; Saiz-Lopez, A.; Thornton, J. A.; Von Glasow, R. Tropospheric Halogen Chemistry: Sources, Cycling, and Impacts. *Chem. Rev.* **2015**, *115*, 4035−4062.
(2) Young, C. J.; Washenfelder, R. A.; Edwards, P. M.; Parrish, D. D.; Gilman, J. B.; Kuster, W. C.; Mielke, L. H.; Osthoff, H. D.; Tsai, C.; Pikelnaya, O.; et al. Chlorine as a Primary Radical: Evaluation of Methods to Understand Its Role in Initiation of Oxidative Cycles. *Atmos. Chem. Phys.* **2014**, *14*, 3427−3440.
(3) Wang, D. S.; Hildebrandt Ruiz, L. Chlorine-initiated oxidation of n-alkanes under high-NO_x conditions: insights into secondary organic aerosol composition and volatility using a FIGAERO-CIMS. *Atmos. Chem. Phys.* **2018**, *18*, 15535−15553.
(4) Sarwar, G.; Simon, H.; Xing, J.; Mathur, R. Importance of Tropospheric $ClNO_2$ Chemistry across the Northern Hemisphere. *Geophys. Res. Lett.* **2014**, *41*, 4050−4058.
(5) Riedel, T. P.; Bertram, T. H.; Crisp, T. A.; Williams, E. J.; Lerner, B. M.; Vlasenko, A.; Li, S.-M.; Gilman, J.; De Gouw, J.; Bon, D. M.; et al. Nitryl Chloride and Molecular Chlorine in the Coastal Marine Boundary Layer. *Environ. Sci. Technol.* **2012**, *46*, 10463−10470.
(6) Mielke, L. H.; Stutz, J.; Tsai, C.; Hurlock, S. C.; Roberts, J. M.; Veres, P. R.; Froyd, K. D.; Hayes, P. L.; Cubison, M. J.; Jimenez, J. L.; et al. Heterogeneous Formation of Nitryl Chloride and Its Role as a Nocturnal NO_x Reservoir Species during CalNex-LA 2010. *J. Geophys. Res.: Atmos.* **2013**, *118*, 10638−10652.
(7) Wang, T.; Tham, Y. J.; Xue, L.; Li, Q.; Zha, Q.; Wang, Z.; Poon, S. C. N.; Dubé, W. P.; Blake, D. R.; Louie, P. K. K.; et al. Observations of Nitryl Chloride and Modeling Its Source and Effect on Ozone in the Planetary Boundary Layer of Southern China. *J. Geophys. Res.: Atmos.* **2016**, *121*, 2476−2489.
(8) Osthoff, H. D.; Roberts, J. M.; Ravishankara, A. R.; Williams, E. J.; Lerner, B. M.; Sommariva, R.; Bates, T. S.; Coffman, D.; Quinn, P. K.; Dibb, J. E.; et al. High Levels of Nitryl Chloride in the Polluted Subtropical Marine Boundary Layer. *Nat. Geosci.* **2008**, *1*, 324−328.
(9) Bannan, T. J.; Booth, A. M.; Bacak, A.; Muller, J. B. A.; Leather, K. E.; Le Breton, M.; Jones, B.; Young, D.; Coe, H.; Allan, J.; et al. The First UK Measurements of Nitryl Chloride Using a Chemical Ionization Mass Spectrometer in Central London in the Summer of 2012, and an Investigation of the Role of Cl Atom Oxidation. *J. Geophys. Res.: Atmos.* **2015**, *120*, 5638−5657.
(10) Haskins, J. D.; Jaeglé, L.; Shah, V.; Lee, B. H.; Lopez-Hilfiker, F. D.; Campuzano-Jost, P.; Schroder, J. C.; Day, D. A.; Guo, H.; Sullivan, A. P.; et al. Wintertime Gas-Particle Partitioning and Speciation of Inorganic Chlorine in the Lower Troposphere over the Northeast United States and Coastal Ocean. *J. Geophys. Res.: Atmos.* **2018**, *123*, 1−20.
(11) Kercher, J. P.; Riedel, T. P.; Thornton, J. A. Chlorine Activation by N_2O_5: Simultaneous, in Situ Detection of $ClNO_2$ and N_2O_5 by Chemical Ionization Mass Spectrometry. *Atmos. Meas. Tech.* **2009**, *2*, 193−204.
(12) Mielke, L. H.; Furgeson, A.; Osthoff, H. D. Observation of $ClNO_2$ in a Mid-Continental Urban Environment. *Environ. Sci. Technol.* **2011**, *45*, 8889−8896.
(13) Mielke, L. H.; Furgeson, A.; Odame-ankrah, C. A.; Osthoff, H. D. Ubiquity of $ClNO_2$ in the Urban Boundary Layer of Calgary, Alberta, Canada. *Can. J. Chem.* **2016**, *94*, 414−423.
(14) Thornton, J. A.; Kercher, J. P.; Riedel, T. P.; Wagner, N. L.; Cozic, J.; Holloway, J. S.; Dubé, W. P.; Wolfe, G. M.; Quinn, P. K.; Middlebrook, A. M.; et al. A Large Atomic Chlorine Source Inferred from Mid-Continental Reactive Nitrogen Chemistry. *Nature* **2010**, *464*, 271−274.
(15) McNamara, S. M.; Kolesar, K. R.; Wang, S.; Kirpes, R. M.; May, N. W.; Gunsch, M. J.; Cook, R. D.; Fuentes, J. D.; Hornbrook, R. S.; Apel, E. C.; et al. Observation of Road Salt Aerosol Driving Inland Wintertime Atmospheric Chlorine Chemistry. *ACS Cent. Sci.* **2020**, *6*, 684−694.
(16) Mitroo, D.; Gill, T. E.; Haas, S.; Pratt, K. A.; Gaston, C. J. $ClNO_2$ Production from N_2O_5 Uptake on Saline Playa Dusts: New Insights into Potential Inland Sources of $ClNO_2$. *Environ. Sci. Technol.* **2019**, *53*, 7442−7452.
(17) Riedel, T. P.; Wagner, N. L.; Dubé, W. P.; Middlebrook, A. M.; Young, C. J.; Öztürk, F.; Bahreini, R.; Vandenboer, T. C.; Wolfe, D. E.; Williams, E. J.; et al. Chlorine Activation within Urban or Power Plant Plumes: Vertically Resolved $ClNO_2$ and Cl_2 Measurements from a Tall Tower in a Polluted Continental Setting. *J. Geophys. Res.: Atmos.* **2013**, *118*, 8702−8715.
(18) Kim, M. J.; Farmer, D. K.; Bertram, T. H. A Controlling Role for the Air-Sea Interface in the Chemical Processing of Reactive Nitrogen in the Coastal Marine Boundary Layer. *Proc. Natl. Acad. Sci. U.S.A.* **2014**, *111*, 3943−3948.
(19) Baergen, A. M.; Styler, S. A.; Van Pinxteren, D.; Müller, K.; Herrmann, H.; Donaldson, D. J. Chemistry of Urban Grime: Inorganic Ion Composition of Grime vs Particles in Leipzig, Germany. *Environ. Sci. Technol.* **2015**, *49*, 12688−12696.
(20) Baergen, A. M.; Donaldson, D. J. Seasonality of the Water-Soluble Inorganic Ion Composition and Water Uptake Behavior of Urban Grime. *Environ. Sci. Technol.* **2019**, *53*, 5671−5677.
(21) Lopez-Hilfiker, F. D.; Constantin, K.; Kercher, J. P.; Thornton, J. A. Temperature Dependent Halogen Activation by N_2O_5 Reactions on Halide-Doped Ice Surfaces. *Atmos. Chem. Phys.* **2012**, *12*, 5237−5247.
(22) Tolbert, M. A.; Rossi, M. J.; Golden, D. M. Antarctic Ozone Depletion Chemistry: Reactions of N_2O_5 with H_2O and HCl on Ice Surfaces. *Science* **1988**, *240*, 1018−1021.

(23) Leu, M.-T. Heterogeneous Reactions of N_2O_5 with H_2O and HCl on Ice Surfaces: Implications for Antarctic Ozone Depletion. *Geophys. Res. Lett.* **1988**, *15*, 851−854.
(24) Domine, F.; Sparapani, R.; Ianniello, A.; Beine, H. J. The Origin of Sea Salt in Snow on Arctic Sea Ice and in Coastal Regions. *Atmos. Chem. Phys.* **2004**, *4*, 2259−2271.
(25) Suzuki, K. Spatial Distribution of Chloride and Sulfate in the Snow Cover in Sapporo, Japan. *Atmos. Environ.* **1987**, *21*, 1773−1778.
(26) Pratt, K. A.; Custard, K. D.; Shepson, P. B.; Douglas, T. A.; Pöhler, D.; General, S.; Zielcke, J.; Simpson, W. R.; Platt, U.; Tanner, D. J.; et al. Photochemical Production of Molecular Bromine in Arctic Surface Snowpacks. *Nat. Geosci.* **2013**, *6*, 351−356.
(27) Custard, K. D.; Raso, A. R. W.; Shepson, P. B.; Staebler, R. M.; Pratt, K. A. Production and Release of Molecular Bromine and Chlorine from the Arctic Coastal Snowpack. *ACS Earth Space Chem.* **2017**, *1*, 142−151.
(28) Raso, A. R. W.; Custard, K. D.; May, N. W.; Tanner, D.; Newburn, M. K.; Walker, L.; Moore, R. J.; Huey, L. G.; Alexander, L.; Shepson, P. B.; et al. Active Molecular Iodine Photochemistry in the Arctic. *Proc. Natl. Acad. Sci. U.S.A.* **2017**, *114*, 10053−10058.
(29) Bartels-Rausch, T.; Jacobi, H.-W.; Kahan, T. F.; Thomas, J. L.; Thomson, E. S.; Abbatt, J. P. D.; Ammann, M.; Blackford, J. R.; Bluhm, H.; Boxe, C.; et al. A Review of Air-Ice Chemical and Physical Interactions (AICI): Liquids, Quasi-Liquids, and Solids in Snow. *Atmos. Chem. Phys.* **2014**, *14*, 1587−1633.
(30) McNamara, S. M.; Raso, A. R. W.; Wang, S.; Thanekar, S.; Boone, E. J.; Kolesar, K. R.; Peterson, P. K.; Simpson, W. R.; Fuentes, J. D.; Shepson, P. B.; et al. Springtime Nitrogen Oxide-Influenced Chlorine Chemistry in the Coastal Arctic. *Environ. Sci. Technol.* **2019**, *53*, 8057−8067.
(31) Apodaca, R. L.; Huff, D. M.; Simpson, W. R. The Role of Ice in N_2O_5 Heterogeneous Hydrolysis at High Latitudes. *Atmos. Chem. Phys.* **2008**, *8*, 12595−12624.
(32) Huff, D. M.; Joyce, P. L.; Fochesatto, G. J.; Simpson, W. R. Deposition of Dinitrogen Pentoxide, N_2O_5, to the Snowpack at High Latitudes. *Atmos. Chem. Phys.* **2011**, *11*, 4929−4938.
(33) Joyce, P. L.; von Glasow, R.; Simpson, W. R. The Fate of NO_x Emissions Due to Nocturnal Oxidation at High Latitudes: 1-D Simulations and Sensitivity Experiments. *Atmos. Chem. Phys.* **2014**, *14*, 7601−7616.
(34) Breining, G. We're pouring millions of tons of salt on roads each winter. Here's why that's a problem. https://ensia.com/features/road-salt/ (accessed Sept 18, 2019).
(35) Kolesar, K. R.; Mattson, C. N.; Peterson, P. K.; May, N. W.; Prendergast, R. K.; Pratt, K. A. Increases in Wintertime $PM_{2.5}$ Sodium and Chloride Linked to Snowfall and Road Salt Application. *Atmos. Environ.* **2018**, *177*, 195−202.
(36) Lilek, J. *Roadway deicing in the United States, Factsheet*, 2017. https://www.americangeosciences.org/critical-issues/factsheet/roadway-deicing-united-states.
(37) Ramakrishna, D. M.; Viraraghavan, T. Environmental Impact of Chemical Deicers - A Review. *Water, Air, Soil Pollut.* **2005**, *166*, 49−63.
(38) Denby, B. R.; Ketzel, M.; Ellermann, T.; Stojiljkovic, A.; Kupiainen, K.; Niemi, J. V.; Norman, M.; Johansson, C.; Gustafsson, M.; Blomqvist, G.; et al. Road Salt Emissions: A Comparison of Measurements and Modelling Using the NORTRIP Road Dust Emission Model. *Atmos. Environ.* **2016**, *141*, 508−522.
(39) Sansalone, J. J.; Glenn, D. W. Accretion of Pollutants in Snow Exposed to Urban Traffic and Winter Storm Maintenance Activities. I. *J. Environ. Eng.* **2002**, *128*, 151−166.
(40) Blomqvist, G.; Johansson, E.-L. Airborne Spreading and Deposition of De-Icing Salt - A Case Study. *Sci. Total Environ.* **1999**, *235*, 161−168.
(41) Labadia, C. F.; Buttle, J. M. Road Salt Accumulation in Highway Snow Banks and Transport through the Unsaturated Zone of the Oak Ridges Moraine, Southern Ontario. *Hydrol. Processes* **1996**, *10*, 1575−1589.
(42) Denby, B. R.; Kupiainen, K. J.; Gustafsson, M. Review of Road Dust Emissions. *Non-Exhaust Emissions: An Urban Air Quality Problem for Public Health; Impact and Mitigation Measures*; Elsevier Inc., 2018; pp 183−203.
(43) Lazarcik, J.; Dibb, J. E. Evidence of Road Salt in New Hampshire's Snowpack Hundreds of Meters from Roadways. *Geosciences* **2017**, *7*, 54.
(44) Wang, S.; McNamara, S. M.; Kolesar, K. R.; May, N. W.; Fuentes, J. D.; Cook, R. D.; Gunsch, M. J.; Mattson, C. N.; Hornbrook, R. S.; Apel, E. C.; et al. Urban Snowpack $ClNO_2$ Production and Fate: A One-Dimensional Modeling Study. *ACS Earth Space Chem.* **2020**, *4*, 1140−1148.
(45) Chang, W. L.; Bhave, P. V.; Brown, S. S.; Riemer, N.; Stutz, J.; Dabdub, D. Heterogeneous Atmospheric Chemistry, Ambient Measurements, and Model Calculations of N_2O_5: A Review. *Aerosol Sci. Technol.* **2011**, *45*, 665−695.
(46) Atkinson, R.; Baulch, D. L.; Cox, R. A.; Crowley, J. N.; Hampson, R. F.; Hynes, R. G.; Jenkin, M. E.; Rossi, M. J.; Troe, J. Evaluated kinetic and photochemical data for atmospheric chemistry: Volume II—gas phase reactions of organic species. *Atmos. Chem. Phys.* **2006**, *6*, 3625−4055.
(47) Wallington, T. J.; Skewes, L. M.; Siegl, W. O. Kinetics of the Gas Phase Reaction of Chlorine Atoms with a Series of Alkenes, Alkynes and Aromatic Species at 295 K. *J. Photochem. Photobiol., A* **1988**, *45*, 167−175.
(48) Sherwen, T.; Schmidt, J. A.; Evans, M. J.; Carpenter, L. J.; Großmann, K.; Eastham, S. D.; Jacob, D. J.; Dix, B.; Koenig, T. K.; Sinreich, R.; et al. Global Impacts of Tropospheric Halogens (Cl, Br, I) on Oxidants and Composition in GEOS-Chem. *Atmos. Chem. Phys.* **2016**, *16*, 12239−12271.
(49) Haskins, J. D.; Lopez-Hilfiker, F. D.; Lee, B. H.; Shah, V.; Wolfe, G. M.; DiGangi, J.; Fibiger, D.; McDuffie, E. E.; Veres, P.; Schroder, J. C.; et al. Anthropogenic Control Over Wintertime Oxidation of Atmospheric Pollutants. *Geophys. Res. Lett.* **2019**, *46*, 14826−14835.
(50) Lelieveld, J.; Gromov, S.; Pozzer, A.; Taraborrelli, D. Global Tropospheric Hydroxyl Distribution, Budget and Reactivity. *Atmos. Chem. Phys.* **2016**, *16*, 12477−12493.
(51) Chen, Q.; Edebeli, J.; McNamara, S. M.; Kulju, K. D.; May, N. W.; Bertman, S. B.; Thanekar, S.; Fuentes, J. D.; Pratt, K. A. HONO, Particulate Nitrite, and Snow Nitrite at a Midlatitude Urban Site during Wintertime. *ACS Earth Space Chem.* **2019**, *3*, 811−822.
(52) Michoud, V.; Doussin, J.-F.; Colomb, A.; Afif, C.; Borbon, A.; Camredon, M.; Aumont, B.; Legrand, M.; Beekmann, M. Strong HONO Formation in a Suburban Site during Snowy Days. *Atmos. Environ.* **2015**, *116*, 155−158.
(53) Sommariva, R.; Crilley, L. R.; Ball, S. M.; Cordell, R. L.; Hollis, L. D. J.; Bloss, W. J.; Monks, P. S. Enhanced Wintertime Oxidation of VOCs via Sustained Radical Sources in the Urban Atmosphere. *Environ. Pollut.* **2021**, *274*, 116563.
(54) Liao, J.; Sihler, H.; Huey, L. G.; Neuman, J. A.; Tanner, D. J.; Friess, U.; Platt, U.; Flocke, F. M.; Orlando, J. J.; Shepson, P. B.; et al. A Comparison of Arctic BrO Measurements by Chemical Ionization Mass Spectrometry and Long Path-Differential Optical Absorption Spectroscopy. *J. Geophys. Res.: Atmos.* **2011**, *116*, D00R02.
(55) De Laeter, J. R.; Böhlke, J. K.; De Bièvre, P.; Hidaka, H.; Peiser, H. S.; Rosman, K. J. R.; Taylor, P. D. P. Atomic weights of the elements. Review 2000 (IUPAC Technical Report). *Pure Appl. Chem.* **2003**, *75*, 683−800.
(56) Eisele, F. L.; Mauldin, R. L.; Tanner, D. J.; Fox, J. R.; Mouch, T.; Scully, T. An Inlet/Sampling Duct for Airborne OH and Sulfuric Acid Measurements. *J. Geophys. Res.: Atmos.* **1997**, *102*, 27993−28001.
(57) Huey, L. G.; Tanner, D. J.; Slusher, D. L.; Dibb, J. E.; Arimoto, R.; Chen, G.; Davis, D.; Buhr, M. P.; Nowak, J. B.; Mauldin, R. L.; et al. CIMS Measurements of HNO_3 and SO_2 at the South Pole during ISCAT 2000. *Atmos. Environ.* **2004**, *38*, 5411−5421.
(58) Guimbaud, C.; Grannas, A. M.; Shepson, P. B.; Fuentes, J. D.; Boudries, H.; Bottenheim, J. W.; Dominé, F.; Houdier, S.; Perrier, S.;

Biesenthal, T. B.; et al. Snowpack Processing of Acetaldehyde and Acetone in the Arctic Atmospheric Boundary Layer. *Atmos. Environ.* **2002**, *36*, 2743−2752.
(59) Dabberdt, W. F.; Lenschow, D. H.; Horst, T. W.; Zimmerman, P. R.; Oncley, S. P.; Delany, A. C. Atmosphere-Surface Exchange Measurements. *Science* **1993**, *260*, 1472−1481.
(60) Fuentes, J. D.; Wang, D.; Neumann, H. H.; Gillespie, T. J.; Den Hartog, G.; Dann, T. F. Ambient Biogenic Hydrocarbons and Isoprene Emissions from a Mixed Deciduous Forest. *J. Atmos. Chem.* **1996**, *25*, 67−95.
(61) Incropera, F. P.; DeWitt, D. P. *Fundamentals of Heat and Mass Transfer*, 3rd ed.; John Wiley & Sons, 1990.
(62) Tang, M. J.; Cox, R. A.; Kalberer, M. Compilation and Evaluation of Gas Phase Diffusion Coefficients of Reactive Trace Gases in the Atmosphere: Volume 1. Inorganic Compounds. *Atmos. Chem. Phys.* **2014**, *14*, 9233−9247.
(63) Monin, A. S.; Obukhov, A. M. Basic Laws of Turbulent Mixing in the Surface Layer of the Atmosphere. *Tr. Akad. Nauk SSSR Geophiz. Inst.* **1954**, *24*, 163−187.
(64) Businger, J. A.; Wyngaard, J. C.; Izumi, Y.; Bradley, E. F. Flux-Profile Relationships in the Atmospheric Surface Layer. *J. Atmos. Sci.* **1971**, *28*, 181−189.
(65) Holtslag, A. A. M.; De Bruin, H. A. R. Applied Modeling of the Nighttime Surface Energy Balance over Land. *J. Appl. Meteorol.* **1988**, *27*, 689−704.
(66) Stull, R. B. *An Introduction to Boundary Layer Meteorology*; Kluwer Academic Publishers: Norwell, MA, 1988.
(67) Honrath, R. E.; Peterson, M. C.; Dziobak, M. P.; Dibb, J. E.; Arsenault, M. A.; Green, S. A. Release of NO_x from sunlight-irradiated midlatitude snow. *Geophys. Res. Lett.* **2000**, *27*, 2237−2240.
(68) Wren, S. N.; Donaldson, D. J.; Abbatt, J. P. D. Photochemical Chlorine and Bromine Activation from Artificial Saline Snow. *Atmos. Chem. Phys.* **2013**, *13*, 9789−9800.
(69) Ahern, A. T.; Goldberger, L.; Jahl, L.; Thornton, J.; Sullivan, R. C. Production of N_2O_5 and $ClNO_2$ through Nocturnal Processing of Biomass-Burning Aerosol. *Environ. Sci. Technol.* **2018**, *52*, 550−559.
(70) Ayers, J. D.; Simpson, W. R. Measurements of N_2O_5 near Fairbanks, Alaska. *J. Geophys. Res.: Atmos.* **2006**, *111*, D14309.
(71) Stutz, J.; Alicke, B.; Ackermann, R.; Geyer, A.; White, A.; Williams, E. J. Vertical Profiles of NO_3, N_2O_5, O_3, and NO_x in the Nocturnal Boundary Layer: 1. Observations during the Texas Air Quality Study 2000. *J. Geophys. Res.: Atmos.* **2004**, *109*, 1−15.
(72) Seok, B.; Helmig, D.; Liptzin, D.; Williams, M. W.; Vogel, C. S. Snowpack-Atmosphere Gas Exchanges of Carbon Dioxide, Ozone, and Nitrogen Oxides at a Hardwood Forest Site in Northern Michigan. *Elementa* **2015**, *3*, 1−20.
(73) Helmig, D.; Boylan, P.; Johnson, B.; Oltmans, S.; Fairall, C.; Staebler, R.; Weinheimer, A.; Orlando, J.; Knapp, D. J.; Montzka, D. D.; et al. Ozone Dynamics and Snow-Atmosphere Exchanges during Ozone Depletion Events at Barrow, Alaska. *J. Geophys. Res.: Atmos.* **2012**, *117*, D20303.
(74) Grannas, A. M.; Jones, A. E.; Dibb, J.; Ammann, M.; Anastasio, C.; Beine, H. J.; Bergin, M.; Bottenheim, J.; Boxe, C. S.; Carver, G.; et al. An Overview of Snow Photochemistry: Evidence, Mechanisms and Impacts. *Atmos. Chem. Phys.* **2007**, *7*, 4329−4373.
(75) Cho, H.; Shepson, P. B.; Barrie, L. A.; Cowin, J. P.; Zaveri, R. NMR Investigation of the Quasi-Brine Layer in Ice/Brine Mixtures. *J. Phys. Chem. B* **2002**, *106*, 11226−11232.
(76) McCaslin, L. M.; Johnson, M. A.; Gerber, R. B. Mechanisms and Competition of Halide Substitution and Hydrolysis in Reactions of N_2O_5 with Seawater. *Sci. Adv.* **2019**, *5*, No. eaav6503.
(77) Transportation Data Management System; Michigan Department of Transportation (MDOT). https://mdot.ms2soft.com/tcds/tsearch.asp?loc=Mdot&mod= (accessed March 16, 2018).
(78) Riedel, T. P.; Bertram, T. H.; Ryder, O. S.; Liu, S.; Day, D. A.; Russell, L. M.; Gaston, C. J.; Prather, K. A.; Thornton, J. A. Direct N_2O_5 Reactivity Measurements at a Polluted Coastal Site. *Atmos. Chem. Phys.* **2012**, *12*, 2959−2968.
(79) Bertram, T. H.; Thornton, J. A. Toward a General Parameterization of N_2O_5 Reactivity on Aqueous Particles: The Competing Effects of Particle Liquid Water, Nitrate and Chloride. *Atmos. Chem. Phys.* **2009**, *9*, 8351−8363.
(80) Finlayson-Pitts, B. J.; Ezell, M. J.; Pitts, J. N. Formation of Chemically Active Chlorine Compounds by Reactions of Atmospheric NaCl Particles with Gaseous N_2O_5 and $ClONO_2$. *Nature* **1989**, *337*, 241−244.
(81) Malley, P. P. A.; Chakraborty, S.; Kahan, T. F. Physical Characterization of Frozen Saltwater Solutions Using Raman Microscopy. *ACS Earth Space Chem.* **2018**, *2*, 702−710.
(82) Morenz, K. J.; Donaldson, D. J. Chemical Morphology of Frozen Mixed Nitrate-Salt Solutions. *J. Phys. Chem. A* **2017**, *121*, 2166−2171.
(83) Colbeck, S. C. An Overview of Seasonal Snow Metamorphism. *Rev. Geophys. Space Phys.* **1982**, *20*, 45−61.
(84) Dominé, F.; Taillandier, A.-S.; Simpson, W. R. A Parameterization of the Specific Surface Area of Seasonal Snow for Field Use and for Models of Snowpack Evolution. *J. Geophys. Res.: Earth Surf.* **2007**, *112*, 1−13.
(85) Burd, J. A.; Peterson, P. K.; Nghiem, S. V.; Perovich, D. K.; Simpson, W. R. Snowmelt onset hinders bromine monoxide heterogeneous recycling in the Arctic. *J. Geophys. Res.: Atmos.* **2017**, *122*, 8297−8309.
(86) Bales, R. C.; Davis, R. E.; Stanley, D. A. Ion Elution through Shallow Homogeneous Snow. *Water Resour. Res.* **1989**, *25*, 1869−1877.
(87) Johannessen, M.; Henriksen, A. Chemistry of Snow Meltwater: Changes in Concentration During Melting. *Water Resour. Res.* **1978**, *14*, 615−619.
(88) Domine, F.; Bock, J.; Voisin, D.; Donaldson, D. J. Can We Model Snow Photochemistry? Problems with the Current Approaches. *J. Phys. Chem. A* **2013**, *117*, 4733−4749.
(89) Edebeli, J.; Trachsel, J. C.; Avak, S. E.; Ammann, M.; Schneebeli, M.; Eichler, A.; Bartels-Rausch, T. Snow Heterogeneous Reactivity of Bromide with Ozone Lost during Snow Metamorphism. *Atmos. Chem. Phys.* **2020**, *20*, 13443−13454.

https://doi.org/10.1021/acsearthspacechem.0c00317
ACS Earth Space Chem. 2021, 5, 1020−1031